On-orbit adjustment calculation for the Generation-X X-ray mirror figure

Daniel A. Schwartz[a], Roger J. Brissenden[a], Martin Elvis[a], Guiseppina Fabbiano[a], Terrance J. Gaetz[a], Diab Jerius[a], Michael Juda[a], Paul B. Reid[a], Scott J. Wolk[a], Stephen L. O'Dell[b], Jeffrey K. Kolodziejczak[b], William W. Zhang[c], and the Generation-X Team.

[a]Harvard-Smithsonian Ctr. for Astrophysics, Cambridge, MA, USA;
[b]NASA/Marshall Space Flight Center;
[c] NASA/Goddard Space Flight Center, Greenbelt, MD, USA

ABSTRACT

Generation-X will be an X-ray observatory with 50 m^2 collecting area at 1 keV and 0.″1 angular resolution. A key concept to enable such a dramatic improvement in angular resolution is that the mirror figure will be adjusted on-orbit; e.g., via piezo-electric actuators deposited on the back side of very thin glass and imparting strains in a bi-morph configuration. To make local adjustments to the individual mirror shells we must employ an imaging detector far forward of the focal surface, so that rays from the individual shells can be measured as distinct rings. We simulate this process on a few representative shells via ray-traces of perfect optics, perturbed axially by low order Legendre polynomial terms. This elucidates some of the requirements for the on-orbit measurements, and on possible algorithms to perform the on-orbit adjustment with acceptably rapid convergence.

Keywords: X-ray telescopes, X-ray optics, Generation-X, figure correction, bi-morph mirrors

1. INTRODUCTION: THE GENERATION-X OBSERVATORY

The Chandra X-ray Observatory represents the state of the art for imaging in X-ray astronomy. *Chandra* provides 0.″5 angular resolution, with about 0.1 m^2 effective area at 1 keV. The next major observatory planned by NASA, *Constellation-X* (Con-X) will have about 30 times more area, motivated, among other objectives, by the need to collect sufficient photons in order to perform high resolution X-ray spectroscopy. Such a dramatic increase of area requires a technology very different from that which resulted in the high resolution of *Chandra* , resulting in a goal of 5″ resolution for that mission. All of the present authors' institutions have been involved in the Con-X studies over the past decade.

X-rays provide a fruitful channel of data about the distant and early universe due to their power to penetrate gas and dust, and to the high efficiency for detecting single photons. To exploit the ultimate information requires still larger collecting area and finer angular resolution. The science goals of detecting the first black holes and galaxies, tracing their evolution from formation to the present epoch, and studying the extreme physics in regions of high mass density, magnetic fields, and kinetic energy flows drive the key parameters for the Generation-X (Gen-X) mission. Of these requirements, the effective area of 50 m^2 and angular resolution of 0.″1 half-power diameter will require the most extensive technology development over the next decade. These developments are influenced and enabled by the experience gained from Con-X, and it is reasonable to assume we will start will a figure quality comparable to the 5″ goal of that mission.

The technology difficulties trace in a major way to the fact that X-rays reflect only at grazing angles. For our concept we will utilize the Wolter I configuration,[1,2] which consists of a paraboloid of revolution followed by a hyperboloid of revolution. Figure 1 illustrates the case of the *Chandra* telescope. For the 0.1 to 10 keV energy range of interest, the appropriate grazing angles are in the range 25′ to 115′. Thus a 50 m^2 collecting area, approximately equivalent to an 8 m diameter telescope, requires instead about 10^4 m^2 collecting area, which would correspond roughly to a 100m diameter normal incidence telescope!

Further author information: (Send correspondence to D.A.S.)
D.A.S.: E-mail: das@head.cfa.harvard.edu

Space Telescopes and Instrumentation 2008: Ultraviolet to Gamma Ray, edited by Martin J. L. Turner, Kathryn A. Flanagan, Proc. of SPIE Vol. 7011, 70110W, (2008) · 0277-786X/08/$18 · doi: 10.1117/12.790085

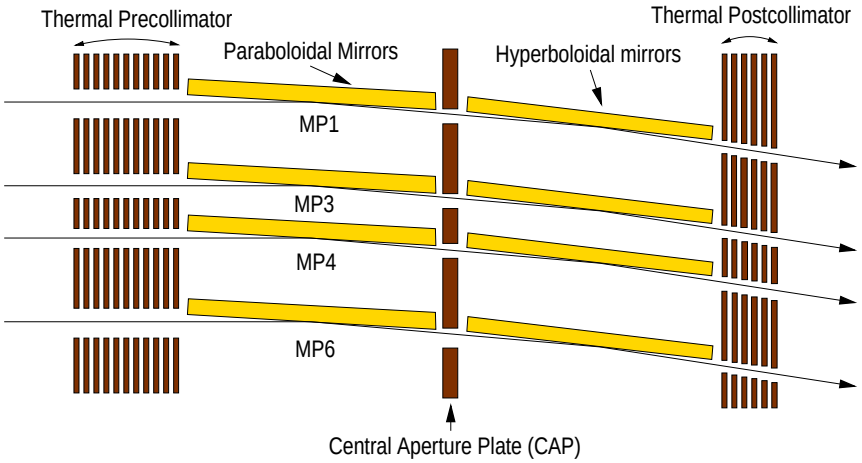

Figure 1. Schematic of the four nested shells which make up the *Chandra* X-ray telescope. The full telescope is rotated about the optical axis, which lies in the plane of the figure 0.6m radius from the outer shell (MP1), and extends through the focus 10m from the central aperture plate. A parallel beam of X-rays from a source at "infinity" are incident from the left, at grazing angles α between $25'$ and $55'$. The effective area is only the sum of the four small rings projected normal to the incident beam. However, the reflecting surfaces which must be precisely figured and polished have $\approx 1/\sin(\alpha) \approx$ 100 times larger area.

With 10^4 m^2 reflecting surface, achieving reasonable launch mass with glass-like materials requires extremely thin shells. To hold the mass down to 5000 to 10000 kg just for the reflectors alone requires thicknesses of only .2 to .4 mm. The geometry requires that the incoming X-rays pass through the spaces between successive shells, so that we are very limited as to what structures we can use to mount and align the shells.

Because of these issues we presume that qualitative improvement over the angular resolution achieved by Con-X will require on-orbit adjustment of the figure. Normal incidence mirrors have successfully used adaptive optics to corrective wavefront distortions induced by the atmosphere. For the grazing incidence application we

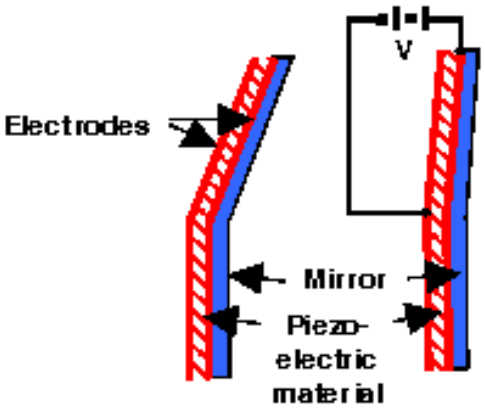

Figure 2. Schematic of the bi-morph adjustment of low frequency slope errors. Applying a voltage across the thin piezo-electric material causes it to expand or contract, imparting a strain which changes the slope of the mirror.

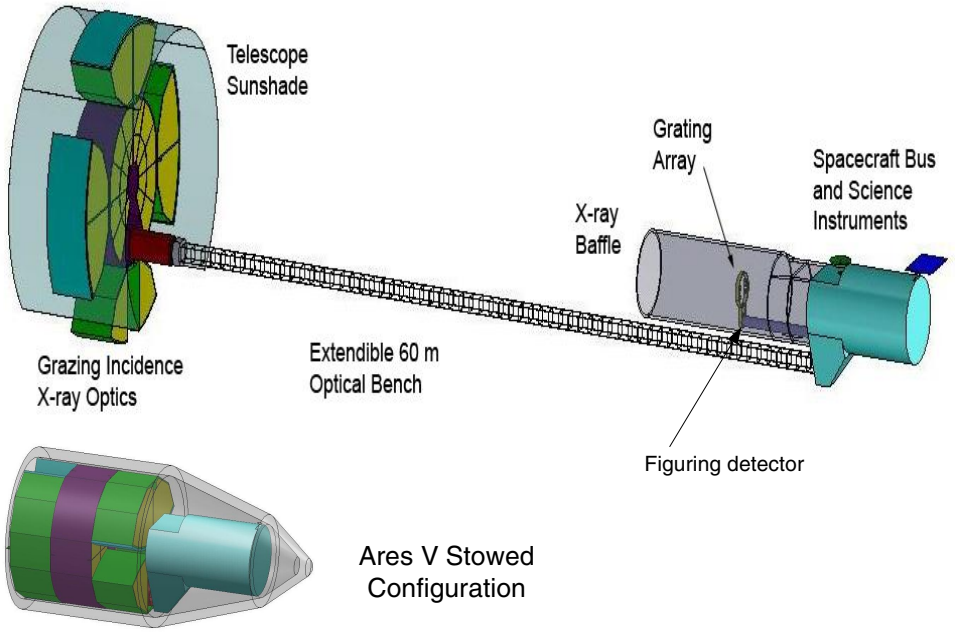

Figure 3. Schematic of stowed (bottom) and deployed (top) configurations of the Gen-X observatory, as enabled by an Ares V with an 8.8m diameter payload capacity. The stowed configuration has a center section which is the 8.3m OD, 3.5m ID filled, central shell, and two petals to each side of this section which unfold at right angles to give a partially filled 16m diameter mirror. The smaller cylinder contains the spacecraft bus and science instruments, and is extended 60m by a truss structure in the on-orbit configuration. The figuring detector to be discussed in this talk conceptually shares structure with the grating array assembly forward of the focal plane.

cannot have a similar approach of actuators which react normal to the reflector as this requires a structure in the optical path between the shells. Instead, for X-ray applications, e.g. at synchrotron facilities,[3,4] a "bi-morph" configuration has been used to impart a strain parallel to the reflecting surface, causing a local change in slope. Figure 2 illustrates the principle. In this figure, thin piezo-electric material is deposited in patches on the back side of the optic. An applied voltage induces strain which can increase or decrease the slope of the reflecting surface.

The telescope assembly itself would be highly segmented, with about 10^4 individual 1m$\times$1m pieces of glass, each figured closely to the desired shape by slumping on an appropriate mandrel, and each piece mounted to a structure. The structures are assembled into modules of various size, and the modules are joined by a deployable, folded structure in order to fit into the fairing of an appropriate launch vehicle. The prospective ARES V launch vehicle provides the capability to carry the complete, stowed observatory to orbit about the L-2 point. Figure 3 shows a concept[5] of Gen-X stowed in the launch configuration, and in the deployed configuration on-orbit.

The on-orbit adjustment of the figure would take place as part of the process of deployment and initial activation. We are considering open-loop processes, where data local to a small azimuthal segment of a specific shell would be acquired and telemetered back to the operations control center, processing and calculations would take place, and adjustment commands would be sent back to the Observatory. This is iterated as needed until the entire telescope is adjusted.

The present paper is an initial exploration of the concept to perform figure adjustment, using observations of a celestial X-ray source. An alternate method might use visible light in a Hartmann test configuration, but with a small aperture that samples a restricted portion of the axial figure. That approach will be investigated elsewhere, as well as an approach combining both methods. We run raytrace simulations of idealized cases, and obtain some parameterized requirements on the detector, mechanism, and data acquisition of the X-ray measurement process. Here we show that the measurement data can give the information required in principle to perform the corrections.

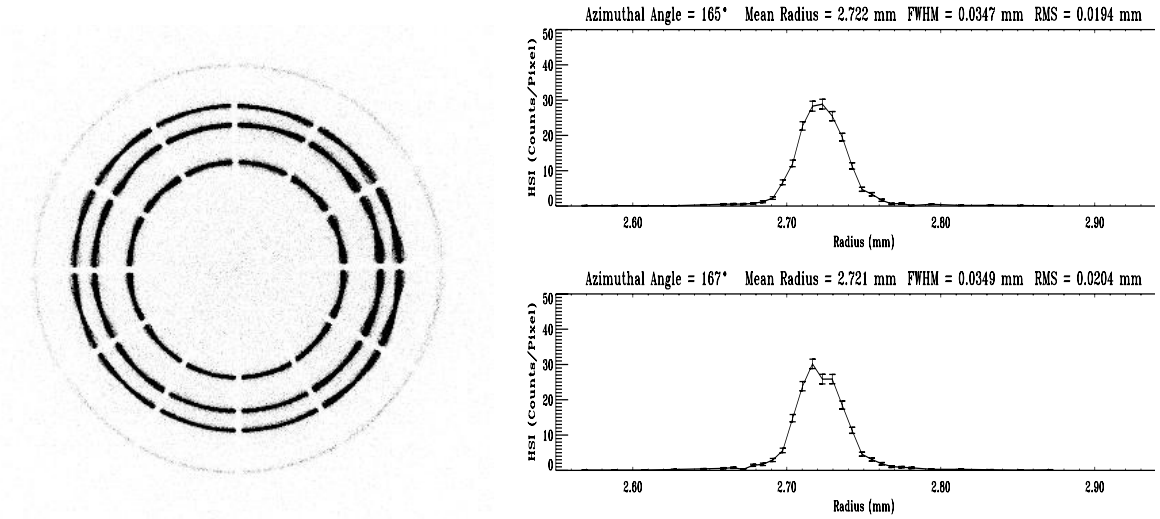

Figure 4. Ground calibration measurements of the ring focus profiles[6] of the *Chandra* Observatory. The left panel shows the image of 6.4 keV X-rays, in a plane 62mm forward of focus, taken in the NASA/MSFC X-ray calibration facility. The outer ring is faint since 6.4 keV is above the critical energy for the grazing angle of this shell. There is a small background due to scattered X-rays. The right panel shows the profile radially across the innermost ring, at two azimuths 2 degrees apart. The mean radius, FWHM, and rms are all within 1 micrometer for the two rings, but there is a small difference in profile shape.

It remains to be shown that an efficient algorithm exists to deduce what mechanical adjustments are to be made, and that mechanical strains can be applied predictably to make the actual adjustment of the mirrors!

2. RING PROFILE MEASUREMENT

The 10^4 individual reflector elements may each require 50 to several hundred piezo actuators to control their shape. To emphasize the obvious, one cannot hope to look at a smeared point source image in the focal plane and make several million adjustments to achieve the best image! Instead, Figure 4 illustrates the kind of data which would be used to provide information for correcting figure errors. The left panel is from a *Chandra* ground calibration image using 6.4 keV Fe-K shell X-rays, taken with a detector about 65 mm forward of the focal plane in the NASA/MSFC X-ray calibration facility. We distinctly see rays from each of the four *Chandra* shells, resolved in azimuth around each shell. Furthermore the radial profile through each shell (right panel), in each azimuth bin, gives information on the axial figure. Although *Chandra* mirrors did not have any adjustment capability, the image clearly shows effects due to gravity and the support flexures, via the increased width around the gaps in the image and especially in the horizontal direction (left and right sides).

The raytrace study reported here had three general objectives: What are the top level requirements on a detector for performing the Gen-X measurements on-orbit, in particular, where would the detector be placed and what are its readout characteristics? Can we use these measurements to detect deviations from the ideal figure at a level which would produce 0.″1 focal plane deviations? Are the measurements practical?

For this study we consider a design with 204 shells of 0.2mm thick glass, with an outer diameter of 16m and inner diameter 3.5m. We only actually work with the two outermost shells, numbers 1 and 2, and two innermost shells, numbers 203 and 204, since those drive the requirements envelope. We consider a Wolter I design, with paraboloidal (P) and hyperboloidal (H) shells each of 1m length, and with a 60m focal length. The shells are spaced to give a 5 arcmin unvignetted field of view, with an additional 10mm clearance between shells. We offset them 25 mm each from the intersection plane.

If we consider 50 actuators along one shell, we might want to measure the profile at 100 independent resolution elements. A detector resolution of 10 micrometers would be reasonable, meaning we need to measure the ring where it is at least 1mm wide. For shell 204 the imager must be at least 8.17m forward of the best focus. This is

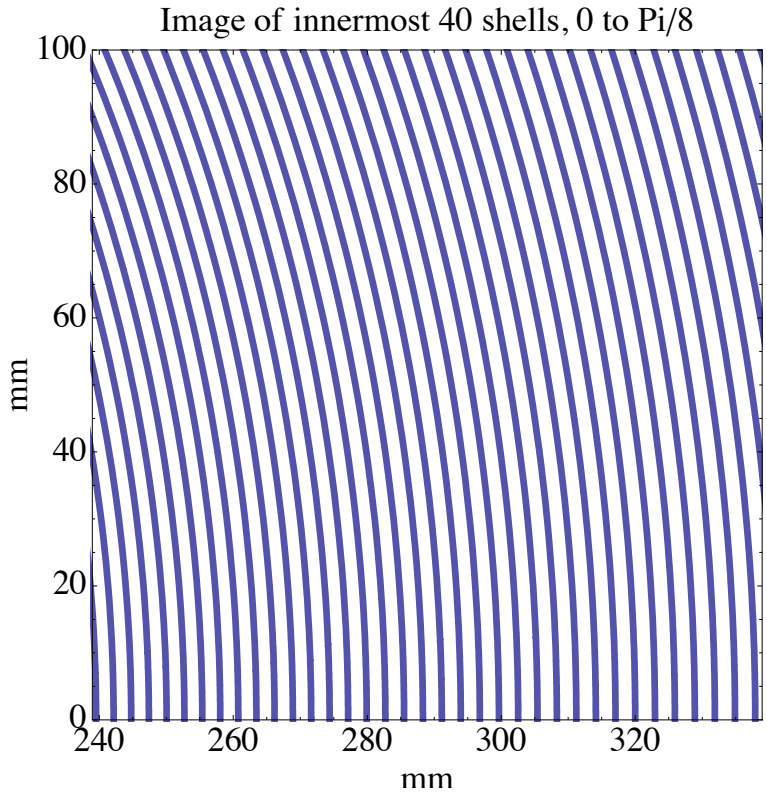

Figure 5. Plot of an azimuthal section of the 40 inner shell ring images, for the case of perfect optics. The figuring detector is located 8,17m forward of the focal plane, so that the ring of the innermost shell is spread by 1mm. The separation of the rings is always greater than this spread, for near-perfect optics.

the most stringent case since the innermost shell has the shallowest grazing angle and therefore the least spread in its converging beam at any axial position. As we can see in Figure 5 we could image about 40 rings in a single imaging detector with a 100mm $\times$ 100mm field. Since the innermost (highest numbered) ring drives the distance at which the ring image detector must be placed, we could use as few as five axial positions, as shown in Figure 6. The imaging detector assembly might have a 2 $\times$ 2 array of detectors, or we might have two assemblies of two detectors each. Allowing for some overlap, each axial position would then involve about 30 azimuthal fields, of which 4 could be measured simultaneously. The actuators might be spaced 2 degrees in azimuth, so we would have 180 $\times$ 204 =36720 ring profiles to be measured. But each would subtend an average of about 1.5 cm^2 (with a factor of few difference inner to outer shell) and would have an average counting rate of 20s^{-1} when pointed at Sco X-1. We could acquire 10^4 counts per ring profile in about 500 s, and if one detector can handle 2 $\times 10^4$ counts s^{-1} an entire measurement series could be obtained in 1/2 day, allowing for 50% duty cycle for positioning and commanding. Conceptually we might forward fit a raytrace model with the amplitudes of 10 to 40 low order polynomial distortions as free parameters, and fit to the 100 bins of each of the 36720 ring profiles. Extrapolation of computational power to the 2020's does not make this a daunting task and even at present it could easily be done with parallel processing; nonetheless, detailed timing studies of an end-to-end correction algorithm need to be done. If we consider this on-orbit adjustment to be part of the mirror manufacturing process, we could afford to spend weeks up to a few months. So iterating by 50 to 100 cycles for the *initial* on-orbit figuring will still be a shorter process than the initial assembly of the mirror shells on the ground. We will expect the figure to remain adjusted for a duration several times longer than the initial adjustment will take. Since subsequent adjustments would take place when (and if) the mirrors just creep beyond the 0.″1 level, we should expect only a few days iteration to restore the image quality.

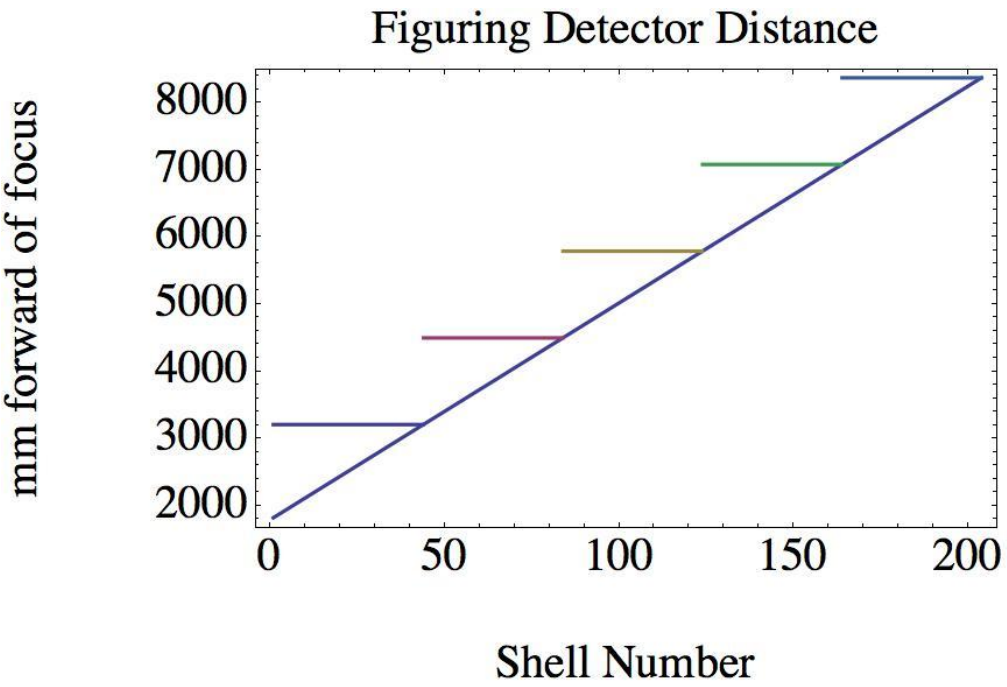

Figure 6. The diagonal line shows the distance forward of focus for which the ring is spread by 1mm width, as a function of shell number. Since we would measure $\approx$ 40 shells at once, the imaging detector would be placed at the five locations shown as horizontal line. In each case it must be placed to accommodate the largest shell number (innermost shell) of the given group.

3. RAY TRACE SIMULATION

We have initially performed idealized ray traces to give a qualitative picture of the on-orbit measurement process. We set up perfect Wolter I geometry, with perfect alignment. We trace only single axial strips, keeping the rays in a two dimensional plane, i.e. with perfect azimuthal geometry and no scattering. The rays are uniformly spaced across the entrance aperture. We introduce low frequency figure errors as Legendre polynomials of order up to 20. This corresponds to spatial frequencies up to 0.02 mm^{-1}, which we expect to be corrected with 20 mm long piezo actuator elements. We later will incorporate realistic actuator effects based on finite element analyses coupled with some laboratory measurements.[7] For the present we are using an artificial model of the actuator corrections.

Figure 7 (left panel) shows the ring profile of a perfect optic. Although this is a trivial raytrace, the key information is that we expect the ring profile to spread from 247.209 to 248.237 mm from the optical axis. If we had used N random rays, instead of an exact uniform spread, we would expect the mean to be determined statistically within $\sqrt{(}1/12N)$, which would be about 3 micrometers for the case N=10,000 shown here. In the right panel we trace 1000 uniform rays, with the paraboloid tilted by 1 micrometer. We still maintain a uniform distribution of rays with each ray just hitting a different hyperboloid element. However, the ring is displaced about 220 micrometers from the perfect case. Such a tilt would produce about 0.″8 blurring in the focal plane, so we need to measure about 20 times better, i.e., to distinguish a 10 micrometer offset. This requires knowledge to better than 10 micrometers for the absolute radial position of the figuring detector.

A key goal of the study was to demonstrate that the ring image could diagnose imperfections at a level relevant to adjusting the image to 0.″1 half-power diameter. Figure 8 demonstrates that this is true. We simulate the distorted figure of both the P and H shells as a sum of Legendre polynomials, with amplitude 0.1/n micrometers, where n=3 to 20 is the Legendre order. This was intended to approximate the power density plot calculated by Reid[8] as the requirement for a corrected Gen-X figure. The raytrace in the focal plane gives an rms image size 0.″21, and a half-power diameter 0.″11. We (unrealistically) set the tilt to zero, so all such plates would contribute

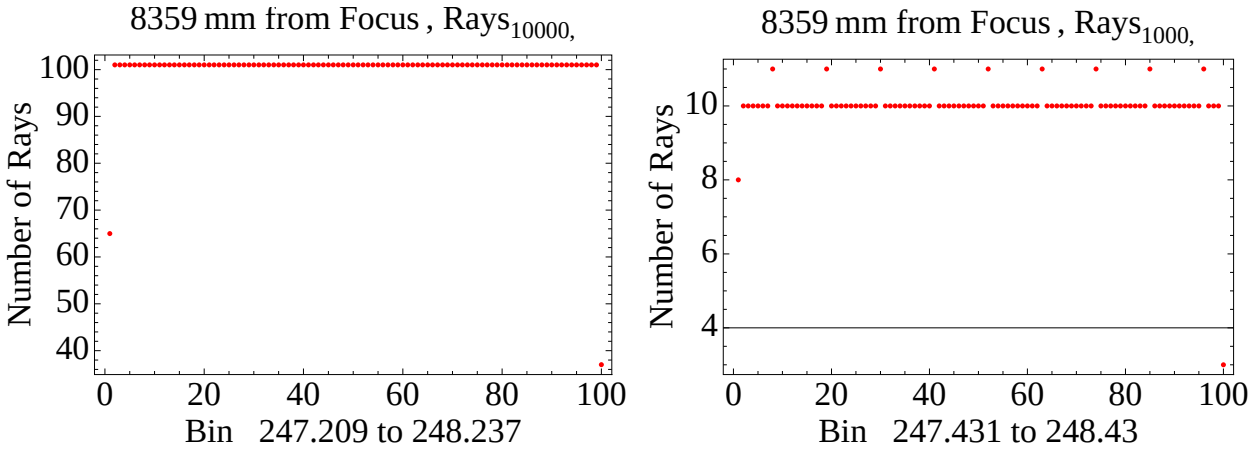

Figure 7. Ring profiles from shell 204 for a perfect optic, (left panel, 10000 rays), and for the paraboloid with a tilt offset of 1 micrometer relative to the hyperboloid (right panel, 1000 rays). The ring distribution is exactly uniform in either case, (binning quantization causes slight deviations at the ends and a "jitter" in the right panel). The key difference is the 220 micrometer displacement of the ring for the tilted case, and this could be easily measured if we have 10 micrometer knowledge of the imaging detector position. The abscissa label gives the span in mm for the distance of bins 1 to 100 relative to the optical axis.

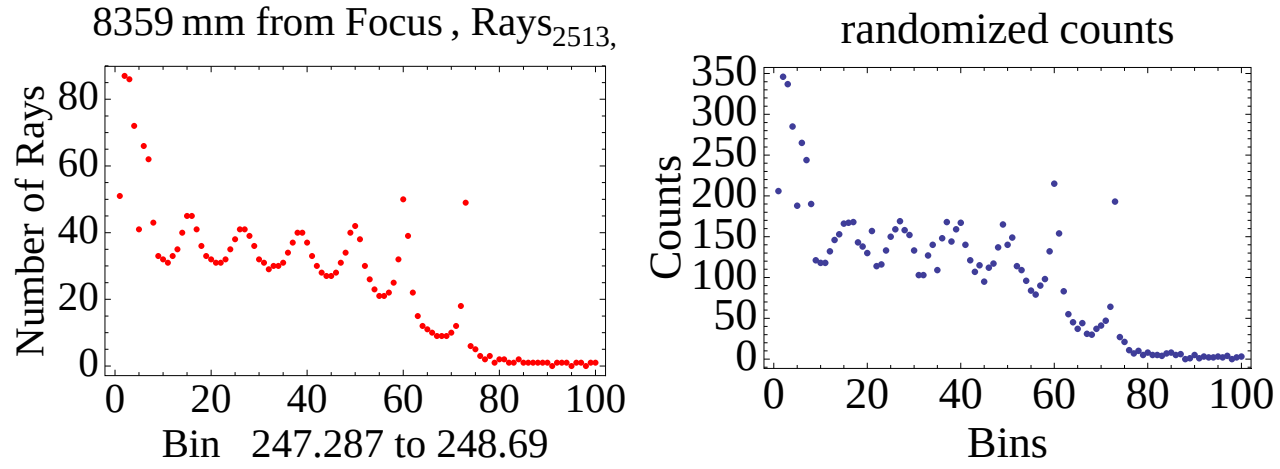

Figure 8. Ring profiles from shell 204 for a distorted optic which would produce a $0\overset{''}{.}21$ image in the focal plane. Left panel: a raytrace with 2500 uniform rays. Right panel: scaling of the raytrace to 10000 rays, and randomizing the counts in each bin for a Poisson distribution.

weighted in root-mean-square by their effective area. The left panel of Figure 8 shows the deterministic raytrace. There is a clear signature of low order slope deviations. In the right panel, we scale the counts to a total of 10,000 rays, and then Poisson randomize the counts in each bin. A signature is still evident. It remains to run candidate correction algorithms on such simulated data to derive a quantitative requirement on the number of counts needed in such an image.

Another diagnostic is given by the overall spread of the ring profile. This is intuitive since large slope errors will cause large deviations of rays. Figure 9 shows overall ring widths increasing from about 6mm to 57mm corresponding to focal plane image sizes from $2\overset{''}{.}2$ to $19''$. These traces were generated by imposing a fourth order Legendre polynomial on the P and H shells, with amplitudes 1, 2.5, 5, and 10 micrometers, respectively, for the increasingly poor images. We should expect that our initial imaging capability prior to adjustment will be at least as good as the Con X telescope capability, which should approach $5''$ at the time the Gen X telescope is being designed. Nonetheless it is not yet clear how poor might be the worst few percent of the approximately 5000 P/H plates comprising the Generation-X telescope assembly.

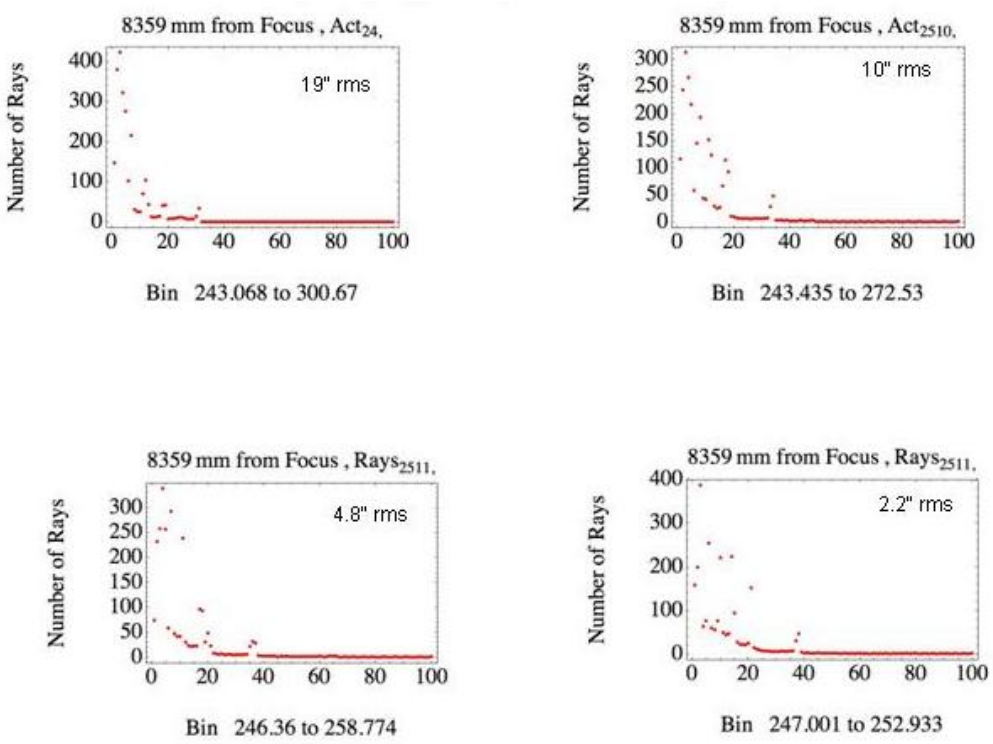

Figure 9. Ring profiles from shell 204 for distorted figures which would produce from 2.″2 to 19″ images in the focal plane. The widths of the rings increase in size from about 6 to 57 mm for these cases.

4. USE OF THE RING PROFILE MEASUREMENTS

The scope of this presentation has been to demonstrate that measurements of the individual ring profiles are feasible, and that they provide relevant diagnostic of the performance in the focal plane. These diagnostics include the ring location, (Figure 7), the detailed ring profile, (Figure 8), and the radial spread of the ring image, (Figure 9). One concept for doing the correction would be to generate raytraces whose free parameters would be the amplitudes of the low order terms in a Fourier or Legendre expansion of the deviations from a perfect surface. The amplitudes would be "best-fit" to the measured ring profiles. Then we would tune the actuators along that axial strip to compensate for the amplitudes we have derived. This derivation may be tricky, since in principle figure deviations on P could be compensated by imposing appropriate figure deviations to H for on-axis rays. In practice it may be extremely unlikely to converge to such a solution, and we will try to assess this with future study. In any event we know the degeneracy can be broken by taking an off-axis measurement, and perhaps by measurement of the same ring at different axial positions.

The actuators must be carefully designed so that they do not merely smooth the deviations at low spatial frequencies and transfer power to higher frequencies where we cannot compensate for rapid changes in slope errors. It is obvious that a "narrow" Gaussian shape does this in principle, since its Fourier transform is a "wide" Gaussian shape. This is just qualitative, and we are working to a practical engineering solution based on the quantitative properties we can establish. Ideally the actuators would simply be low order polynomials in the axial coordinate, and with sufficient dynamic range in amplitude for the necessary corrections.

ACKNOWLEDGMENTS

This work has been supported in part by the National Aeronautics and Space Administration (NASA) contract NAS8-39073 to the Chandra X-ray Center.

REFERENCES

[1] Wolter, H. *Ann. Physik* **10**, 94 (1952).

[2] Wolter, H. *Ann. Physik* **10**, 286 (1952).

[3] Signorato, R., Carre, J.-F., and Ishikawa, T., "Performance of the spring-8 modular piezoelectric bimorph mirror prototype," in [*X-Ray Mirrors, Crystals, and Multilayers*], Freund, A. K. and Ishikawa, T., eds., *Proc. SPIE* **4501**, 76–87 (2001).

[4] Signorato, R., "Modular bimorph mirrors: From an established hardware design to first experimental results towards wavefront correction in the x-ray domain," in [*SYNCHROTRON RADIATION INSTRUMENTATION*], *AIP Conference Proceedings* **705**, 812–818 (2004).

[5] Brissenden, R. J., "Generation-x: a mission enabled by ares v," in [*Ares V - Astronomy Workshop*], (2008).

[6] Zhao, P., Freeman, M., Jerius, D., and Shao, Y., "Axaf veta-i mirror ring focus measurements," in [*Multilayer and Grazing Incidence X-Ray/EUV Optics II*], Hoover, R. B. and Walker, A. B., eds., *Proc. SPIE* **2011**, 59–74 (1994).

[7] Reid, P. B., Davis, W. N., Freeman, M., Juda, M., Podgorski, W. A., and Schwartz, D. A., "Development of adjustable grazing incidence optics for generation-x," in [*Space Telescopes and Instrumentation II: Ultraviolet to Gamma Ray 2008*], Turner, M. J. L. and Flanagan, K. A., eds., *Proc. SPIE* **7011** (2008).

[8] Reid, P. B., Cameron, R. A., Cohen, L., Elvis, M., Gorenstein, P., Jerius, D., Petre, R., Podgorski, W. A., Schwartz, D. A., and Zhang, W. W., "Constellation-x to generation-x: evolution of large collecting area moderate resolution grazing incidence x-ray telescopes to larger area high-resolution adjustable optics," in [*UV and Gamma-Ray Space Telescope Systems.*], Gnther Hasinger, M. J. L. T., ed., *Proc. SPIE* **5488** (2004).